



Photocatalytic decolorization of 5-[4-(dimethylamino)phenylmethylene]-2-thioxo-4-thiazolidinone using nano-powder zinc oxide at various basic buffer pHs

Morteza Montazerzohori*, Sayed Amin Hosseini Pour

Department of Chemistry, Yasouj University, Yasouj 75914-353, Iran

Email: mmzohori@mail.yu.ac.ir

Received 14 April 2013; Accepted 5 August 2013

ABSTRACT

Decolorization of 5-[4-(dimethylamino)phenylmethylene]-2-thioxo-4-thiazolidinone was photocatalyzed by nano-sized zinc oxide at various basic buffer solutions with pHs of 9–13. Various effectual physicochemical parameters such as dye concentration, dosage of photocatalyst, irradiation time, and pH of solution on photocatalytic decolorization under high-pressure mercury lamp illumination were optimized. The dye was found to be decolorized effectively at optimum conditions within 90–180 min. The kinetic studies showed a pseudo-first-order kinetic behavior regarding the Langmuir–Hinshelwood kinetic model at all basic pHs. The pseudo-first-order rate constants (k_{obs}) of photocatalytic process were evaluated in the range of 1.80×10^{-2} – 4.40×10^{-2} for the studied pHs (9, 10, 12, and 13). Furthermore, k_r , rate constant of decolorization at catalyst surface, and K_A , adsorption constants of dye were calculated based on the Langmuir–Hinshelwood model at investigated pHs.

Keywords: Decolorization; Zinc oxide; Nano-structure; Photocatalytic

1. Introduction

At increasing rate at the chemical and food industries causes wide disposal of large amounts of organic pollutants to wastewaters that are responsible for environmental problems [1–6]. These organic pollutants introduce both color and high character of toxicity to receiver water that is harmful to the various aquatic lives in ecosystem. Thus, the treatment of wastewaters is necessary for the removal of any unpleasant parameters. Dye removal is performed by various methods such as dye adsorption by wastewater treatment plant [7,8], coagulation [9,10], floccula-

tion [11,12], ozonation [13], reverse osmosis [14,15] and physical adsorption on some organic or inorganic materials and/or nano-material [16–21]. The above-referred methods are generally non-destructive and in fact transfer the organic pollutants from wastewaters to another place. To overcome this disadvantage, various oxidative degradation methods have been utilized such as advanced oxidation process using UV/H₂O₂ [22,23], photo-Fenton reagent [24,25], and photocatalytic process [26–32]. Finally, for many environmental researchers, complete oxidation of the pollutants to mineralized products is favorite. The air may be considered as a cheap and convenient oxidant in photocatalytic oxidation. The titled dye that is also known as rhodanine may be harmful when it is inhaled,

*Corresponding author.

swallowed, or absorbed through skin, and also it causes irritation of skin and eye. To the best of our knowledge, there is no report on photocatalytic degradation and/or decolorization of the titled dye. In this direction, in continuation of our previous works [33–37], herein we wish to report the photocatalytic degradation of titled dye using nano-sized zinc oxide under aerobic condition in basic buffer solutions.

2. Materials and methods

2.1. Reagents

All chemicals were provided from Merck, Fluka and Aldrich. 5-[4-(dimethylamino)phenylmethylene]-2-thioxo-4-thiazolidinone was purchased from Merck. Nanopowder zinc oxide (<100 nm) was analytical grade with surface area 15–25 m²g⁻¹ (Sigma–Aldrich). The SEM and TEM of nanopowder zinc oxide are shown in Fig. 1. The basic buffer solutions were

prepared by the following compounds: KH₂PO₄, Na₂HPO₄, NaOAc, HOAc, Na₂B₄O₇, HCl, H₂SO₄ and NaOH. Double distilled water was used for preparing the buffer solutions.

2.2. Apparatus

Photochemical apparatus containing 400W high-pressure mercury lamp was used for photocatalytic degradation experiments. UV–visible spectrophotometer, JASCO-V570, was applied for the monitoring of the photoremoval of titled dye. Separation of photocatalyst particles was performed by a centrifuge of Sigma-301 model. The pH of buffer solutions was adjusted by the aid of pH-meter of F-60.

2.3. Determination of residual dye concentration

The concentration of residual dye after each photoprocess was determined by means of calibration curves that have been plotted based on a series of standard solutions with regard to λ_{\max} of titled dye at 455 nm for each solution with pHs of 9, 10, 12, and 13.

2.4. General procedure for photocatalytic dye removal

The photocatalytic removal processes were performed by irradiation of continuously stirred of 25 mL of a buffer solution (pHs of 9, 10, 12, and 13) containing 30 ppm of dye and a considered amount of photocatalyst under air-bubbling conditions by an air pump in photoreactor instrument equipped with 400W high-pressure mercury lamp at room temperature. After definite time for each photoprocess, photocatalyst (nano-powder) was separated by centrifugation of photoirradiated reaction mixture, and then, residual concentration of dye was measured by spectrophotometric method and by the aid of calibration curves at each pH.

3. Results and discussion

3.1. Calibration curves

The solubility of titled dye was not suitable at acidic and neutral media, but it dissolves in basic media well. Therefore, the photocatalytic processes were designed for basic media at pHs of 9–13. The 30 ppm of dye solution at all studied pHs was chosen as target concentration for degradation. Due to high molar absorption coefficient of dye, the use of higher initial concentration was not possible because of the ambiguity that exists in dye removal monitoring by spectrophotometric method during the photo-processes. With regard to initial dye

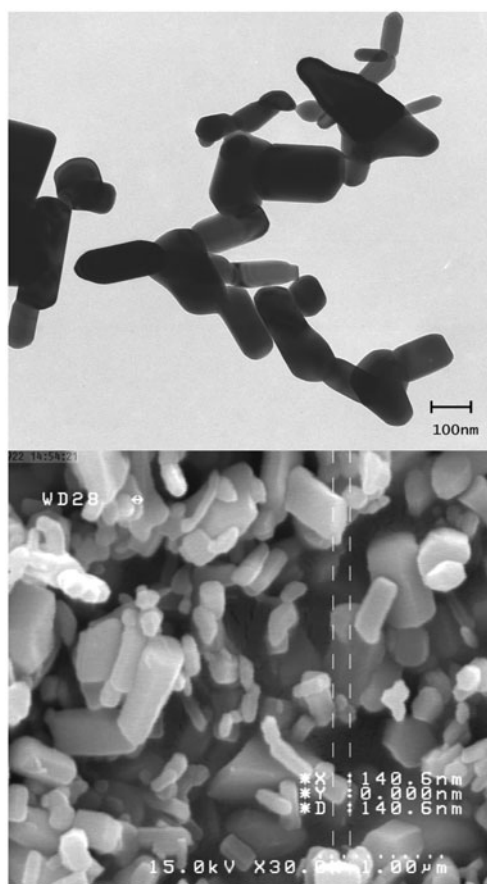


Fig. 1. The TEM and SEM of nanopowder zinc oxide.

concentration in photoprocess, the range of 0–30 ppm of dye solution with pHs of 9–13 was used for plotting the calibration curves as absorbance vs. concentration at $\lambda_{\max} = 455 \text{ nm}$ as shown in Fig. 2.

3.2. Catalyst loading effect

The amount effect of zinc oxide nano-powder on photocatalytic dye removal as diagrams exhibiting dye residual concentration vs. catalyst amount at each pH has been shown in Fig. 3. As shown in Fig. 3, with an increase in catalyst amount, a decrease in residual concentration is observed until after that no higher dye removal or even reverse change is seen. With a focus on the diagrams, it is possible to suggest optimum amounts of photocatalyst at each pH. Accordingly, the selected optimum amounts of catalyst for next processes were considered as 30 mg for pHs of 9 and 12; and 25 mg for pHs of 10 and 13 per 25 mL of solution. This behavior has been observed by the others through photocatalytic degradation reports [38,39]. The decrease in residual concentration with an increase in catalyst amount may be due to an increased number of active sites on zinc oxide nano-powder surface, although, more amount of catalyst than optimum values, may cause light scattering and then reducing the suitable penetration of light to the solution and depress the target excitation of photocatalyst particles leading to decrease in the efficiency of the photoprocess [38–40]. Self-deactivation and agglomeration of the photocatalyst nanoparticles during the irradiation may be considered as other reasons for the observable trends in the diagrams of residual concentration vs. catalyst amount in current photocatalytic degradation [40].

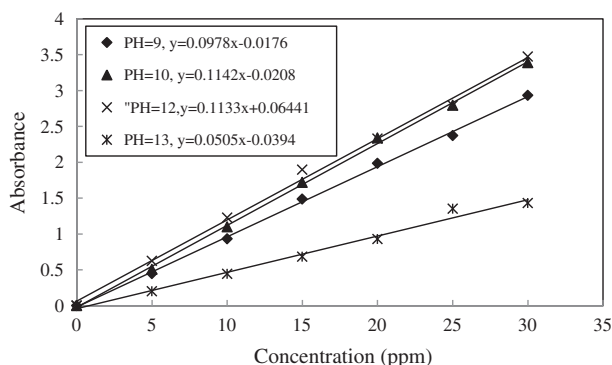


Fig. 2. Calibration curves of dye at various buffer media at 455 nm (pH=9 (◆), pH=10 (▲), pH=12 (×), and pH=13 (*)).

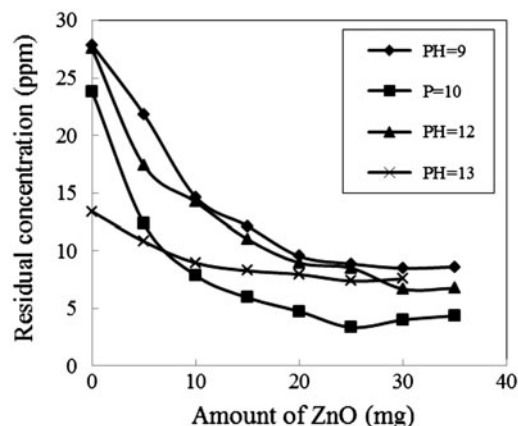


Fig. 3. The effect of nano-catalyst amount on photocatalytic removal (irradiation time = 1 h; $V = 25 \text{ mL}$).

3.3. pH effect

It is obvious that pH has a key role in many types of reactions, especially in photocatalytic treatment of pollutants, so that the scientists in this field generally investigate its effect [26–40]. The effect of pH on dye photocatalytic removal is discussable in several points of view that can be referred to it based on its effect on catalyst surface and probable protonation-deprotonation of dye in bulk solution. In the view of catalyst surface, the pH induces positive, negative, and/or neutral charges to the surface of catalyst. Zinc oxide nano-powder has a nearly neutral surface at pH 8.9 [41]. Above this pH, more negatively charged and below that more positively charged particles exist. The surface charge can effect on the adsorption of dye on it and therefore influences on its photoremoval. On the other hand, the protonation-deprotonation of dye is directly affected by the pH of medium. Although the current photocatalytic degradation had been investigated separately at four buffer pHs, but a competitive photocatalytic removal was designed. For this mean, four photoexperiments using the optimum catalyst amount with pHs of 9, 10, 12, and 13 at the same condition were performed. The results have been presented as column plots showing the photocatalytic degradation (%) vs. pH after 1 h in Fig. 4. As it can be seen from this figure, the higher removal belongs to the pH of 10 and pHs of 12, 9 and 13 are in the next positions, respectively. It is suggested that the dye is in neutral form when pH is 10 while the catalyst surface is nearly negatively charged at this pH. The hydrogen bonding between the NH-group of dye and surface oxide anions of zinc oxide causes the suitable adsorption of dye leading to higher degradation of dye molecules by holes (h+) attack of excited active sites of catalyst at pH=10. At higher pHs, 12 and 13

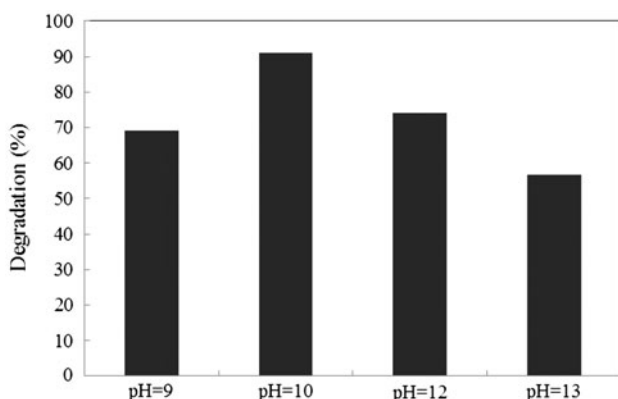


Fig. 4. The effect of pH on photocatalytic degradation (%) (nano-powder ZnO: optimum amount in each pH; $V = 25$ mL; irradiation time = 1 h).

probably dye molecules are deprotonated to anionic forms in bulk solution. Also the catalyst surface is more negatively charged than when pH is equal to 10, and therefore a considerable repulsion between dye anions and negative surface is occurred that causes lower dye adsorption on surface and accordingly a lower degradation is observed. Of course, it is also to be referred that the dye degradation happens both at catalyst surface and in bulk solution. Naturally, in more basic medium, more hydroxyl radical exists due to higher concentration of hydroxide anions that again can effect on the rate of degradation.

3.4. Kinetics investigation

First-order kinetics has been often reported for photocatalytic removal of dyes at various conditions in which the concentration of dye exponentially decreases vs. irradiation time [26–40]. In the current study as shown in Fig. 5, the plots of the residual concentration vs. time are found to be exponentially decreased suggesting first-order kinetics for photocatalytic removal of dye at all studied pHs.

For the evaluation of observed first-order rate constants at various pHs (k_{obs}), the plot of $\ln(C_0/C_t)$ (in which C_0 and C_t are initial dye concentration and concentration at time t , respectively) vs. time (t) were sketched and presented in Fig. 6. It is well exhibited that all diagrams are linear with high regression coefficient (R) so that the slope of the plot at each pH can be evaluated as k_{obs} at that conditions. The observed rate constants at all buffer solutions have been collected at Table 1. The results show that the value of k_{obs} are found in the range of $(1.8\text{--}4.4) \times 10^{-2}$ with an order of degradation for pHs of 10, 12, 9, and 13, respectively. The same explanation as suggested in

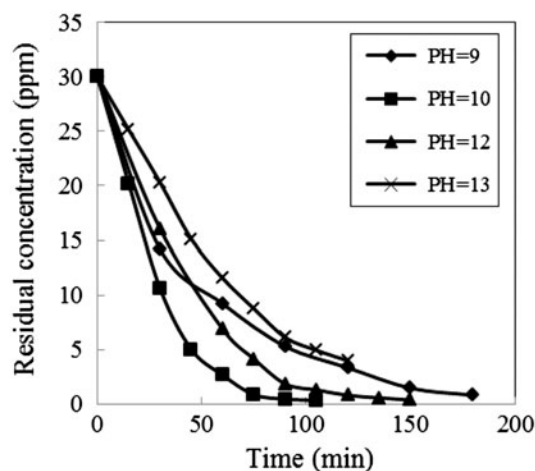


Fig. 5. Residual concentration vs. time during the photocatalytic degradation at various buffer pHs by using optimum amount of zinc oxide nano-powder ($V = 25$ mL).

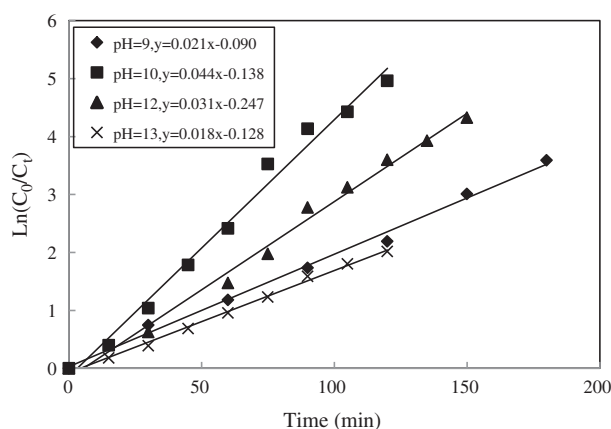


Fig. 6. The plots of $\ln(C_0/C_t)$ vs. time (min) at various buffer pHs for photocatalytic removal of dye.

previous section can be presented for the observed trend in k_{obs} values.

More kinetic investigations were carried out by using Langmuir–Hinshelwood (L–H) model that is presented by equation (Eq. (1)):

$$1/R = 1/k_r K_A [C_0] + 1/k_r \quad (1)$$

where K_A is the adsorption constant, $[C_0]$ is initial concentration of dye, and k_r is apparent degradation rate constant at catalyst surface [42–44]. If the plot of $1/R$ vs. $1/[C_0]$ is drawn and a linear diagram is observed, it indicates the photocatalytic removal is in agreement with L–H model. Thus, the slopes and intercepts values of plots are equal to $1/k_r K_A$ and $1/k_r$, respectively. The related plots for the titled dye in the current work were depicted in Fig. 7.

Table 1
Kinetic and thermodynamic parameters in photodegradation of dye at various buffer pHs

| Parameters | pH=9 | pH=10 | pH=12 | pH=13 |
|--|------------------------|------------------------|-----------------------|-----------------------|
| K_A (L mg ⁻¹) | 7.29×10^{-3} | 7.27×10^{-3} | 1.14×10^{-1} | 4.38×10^{-2} |
| k_r (mg min ⁻¹ L ¹) | 43.29×10^{-1} | 38.46×10^{-1} | 2.06×10^{-1} | 7.50×10^{-1} |
| k_{obs} (min ⁻¹) | 2.1×10^{-2} | 4.4×10^{-2} | 3.1×10^{-2} | 1.8×10^{-2} |
| $t_{1/2}$ (min) | 33.00 | 15.75 | 22.35 | 38.5 |

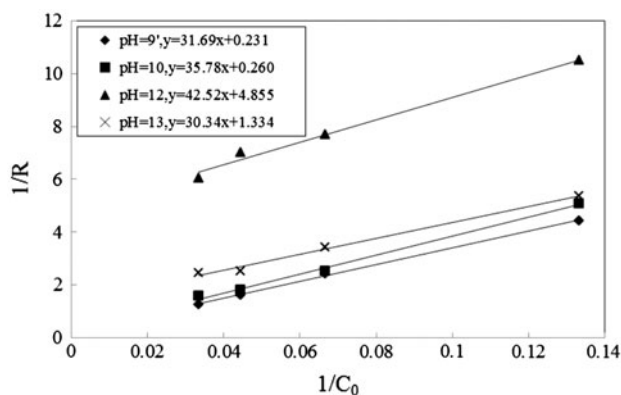


Fig. 7. The plots of $1/R$ vs. $1/C_0$ at various buffer pHs based on L–H model for photocatalytic removal of dye.

The plots in Fig. 7 reveal that the rates vary proportional to the initial dye concentration at various pHs meaning that an increase or decrease causes increase or decrease in rate value. The evaluated k_{obs} , K_A , k_r , and dye degradation half-life ($t_{1/2}$) at various buffer pHs have been tabulated in Table 1.

As seen in Table 1, the L–H rate constant k_r is decreased as the solution pH is raised from 9 to 12 and then smoothly is increases. The minimum and maximum of dye degradation half time, $t_{1/2}$ is belonged to pH=10 and 13, respectively.

4. Conclusion

In this work, we described photocatalytic removal of 5-[4-(dimethylamino) phenylmethylene]-2-thioxo-4-thiazolidinone at various buffer pHs. The effects of some agents such as amount of photocatalyst, pH, and irradiation time were investigated. The maximum of photocatalytic degradation rate was evaluated at pH=10 by using of optimum amount of 25 mg per 25 mL of 30 ppm dye solution in our conditions. The investigation of photocatalytic dye removal based on L–H kinetic model revealed that the photocatalytic process obey from it. Furthermore, the L–H rate constant; k_r , adsorption constant, K_A and dye degradation half time, $t_{1/2}$ were evaluated at different buffer basic media.

Acknowledgment

A partial support of Yasouj University to complete this study is acknowledged.

References

- [1] H.R. Pouretdal, H. Motamedi, A. Amiri, Aromatic compounds photodegradation catalyzed by ZnS and CdS nanoparticles, *Desalin. Water Treat.* 44 (2012) 92–99.
- [2] N. Barco-Bonilla, R. Romero-Gonzalez, P. Plaza-Bolanos, A. Garrido-Frenich, J.L. Martínez Vidal, J.J. Salas, I. Martín, Study of the distribution of 204 organic contaminants between the aqueous phase and the suspended particulate matter in treated wastewater for proper environmental control, *Desalin. Water Treat.* 51 (2013) 2497–2515.
- [3] F.H. Hussien, T.A. Abass, Photocatalytic treatment of textile industrial wastewater, *Int. J. Chem. Sci.* 8 (2010) 1353–1364.
- [4] T. Robinson, G. Mc Mullan, R. Marchant, P. Nigam, Remediation of dyes in textile effluents: A critical review on current treatment technologies with a proposed alternative, *Bioresour. Technol.* 77 (2001) 247–255.
- [5] S. Rodriguez-Couto, M. Sanroman, G.M. Guebitz, Influence of redox mediators and metal ions on synthetic acid dye decolorization by crude laccase from *T. hirsute*, *Chemosphere* 58 (2005) 417–422.
- [6] T.S. Shaffiqu, J.J. Roy, R.A. Nair, T.E. Abraham, Degradation of textile dyes mediated by plant peroxidases, *Appl. Biochem. Biotechnol.* 102–103 (2002) 315–326.
- [7] K.V. Gernaey, M.C.M. Van Loosdrecht, M. Henze, M. Lind, S.B. Jorgensen, Activated sludge wastewater treatment plant modelling and simulation: State of the art, *Environ. Modell. Softw.* 19 (2004) 763–783.
- [8] S. Sadri Moghaddam, M.R. Alavi Moghaddam, M. Arami, Decolorization of an acidic dye from synthetic wastewater by sludge of water treatment plant, Iran. *J. Environ. Health Sci. Eng.* 7 (2010) 437–442.
- [9] Y. Wang, L. Shu, V. Jegatheesan, B. Gao, Coagulation and nano-filtration: A hybrid system for the removal of lower molecular weight organic compounds (LMWOC), *Desalin. Water Treat.* 11 (2009) 23–31.
- [10] B.Y. Gao, Y. Wang, Q.Y. Yue, J.C. Wei, Q. Li, Color removal from simulated dye water and actual textile wastewater using a composite coagulant prepared by polyferric chloride and polydimethylallylammonium chloride, *Sep. Purif. Technol.* 54 (2007) 157–163.
- [11] M.M. Nourouzi, T.G. Chuah, T.S. Choong, Optimisation of reactive dye removal by sequential electrocoagulation-flocculation method: Comparing ANN and RSM prediction, *Water Sci. Technol.* 63 (2011) 984–994.
- [12] S.S. Moghaddam, M.R. Moghaddam, M. Arami, Coagulation/flocculation process for dye removal using sludge from water treatment plant: Optimization through response surface methodology, *J. Hazard. Mater.* 175 (2010) 651–657.
- [13] M. Dudziak, Purification of water containing mycoestrogens using ozonation and nano-filtration, *Desalin. Water Treat.* 48 (2012) 232–237.

- [14] K. Turhan, Z. Turgut, Treatment and degradability of direct dyes in textile wastewater by ozonation: A laboratory investigation, *Desalin. Water Treat.* 11 (2009) 184–191.
- [15] M. Ramesh kumar, K. Saravanan, Application of reverse osmosis membrane system for treatment of effluent in textile knitted fabric dyeing, *Afr. J. Biotechnol.* 10 (2011) 15756–15762.
- [16] O. Yavuz, A.H. Aydin, Removal of direct dyes from aqueous solution using various adsorbents, *Polish J. Environ. Stud.* 15 (2006) 155–161.
- [17] X.-D. Xin, J. Wang, H.-Q. Yu, B. Du, Q. Wei, L.-G. Yan, Removal of o-nitrobenzoic acid by adsorption on to a new organoclay: Montmorillonite modified with HDTMA micro-emulsion, *Desalin. Water Treat.* 32 (2011) 447–454.
- [18] M. Iram, C. Guo, Y. Guan, A. Ishfaq, H. Liu, Adsorption and magnetic removal of neutral red dye from aqueous solution using Fe₃O₄ hollow nanospheres, *J. Hazard. Mater.* 181 (2010) 1039–1050.
- [19] M. Ghaedi, H. Khajehsharifi, A. Hemmati Yadkuria, M. Roostaa, A. Asghari, Oxidized multiwalled carbon nanotubes as efficient adsorbent for bromothymol blue, *Toxicol. Environ. Chem.* 94 (2012) 873–883.
- [20] M. Ghaedi, A. Hekmati Jah, S. Khodadoust, R. Sahraei, A. Daneshfar, A. Mihandoost, M.K. Purkait, Cadmium telluride nanoparticles loaded on activated carbon as adsorbent for removal of sunset yellow, *Spectrochim. Acta A* 90 (2012) 22–27.
- [21] M. Ghaedi, Comparison of cadmium hydroxide nanowires and silver nanoparticles loaded on activated carbon as new adsorbents for efficient removal of Sunset yellow: Kinetics and equilibrium study, *Spectrochim. Acta A* 94 (2012) 346–351.
- [22] C. Li, N.-Y. Gao, W. Li, Photochemical degradation of typical herbicides simazine by UV/H₂O₂ in aqueous solution, *Desalin. Water Treat.* 36 (2011) 197–202.
- [23] E.C. Pires, T.J. Momeni, Combination of an anaerobic process with O₃, UV and O₃/UV for cellulose pulp bleaching effluent treatment, *Desalin. Water Treat.* 5 (2009) 213–222.
- [24] M. Qiu, C. Huang, A comparative study of degradation of the azo dye C.I. Acid Blue 9 by Fenton and photo-Fenton oxidation, *Desalin. Water Treat.* 24 (2010) 273–277.
- [25] S. Adishkumar, S. Sivajothi, J. Rajesh Banu, Coupled solar photo-fenton process with aerobic sequential batch reactor for treatment of pharmaceutical wastewater, *Desalin. Water Treat.* 48 (2012) 89–95.
- [26] M. Montazerzohori, S. Mojahedi Jahromi, Photocatalytic decolorization of ethyl orange at various buffer solutions using nano-titanium dioxide: A kinetic investigation, *Desalin. Water Treat.* 48 (2012) 261–266.
- [27] T. Aye, W.A. Anderson, M. Mehrvar, Photocatalytic treatment of cibacron brilliant yellow 3G-P (reactive yellow 2 textile dye), *J. Environ. Sci. Health. A* 38 (2003) 1903–1914.
- [28] M.G. Neelavannan, M. Revathi, C. Ahmed Basha, Photocatalytic and electrochemical combined treatment of textile wash water, *J. Hazard. Mater.* 149 (2007) 371–378.
- [29] K. Hashimoto, H. Irie, A. Fujishima, TiO₂ Photocatalysis: A historical overview and future prospects, *Japan. J. Appl. Phys.* 44 (2005) 8269–8285.
- [30] K. Rajeshwar, C.R. Chenthamarakshan, S. Goeringer, M. Djukic, Titania-based heterogeneous photocatalysis: Materials, mechanistic issues, and implications for environmental remediation, *Pure Appl. Chem.* 73 (2001) 1849–1860.
- [31] M.H. Habibi, E. Askari, Spectrophotometric studies of photo-induced degradation of tertrodirect light blue (TLB) using a nanostructure zinc zirconate composite, *J. Ind. Eng. Chem.* 19 (2013) 1400–1405.
- [32] M.H. Habibi, R. Sheibani, Nanostructure silver-doped zinc oxide films coating on glass prepared by sol-gel and photochemical deposition process: Application for removal of mercaptan, *J. Ind. Eng. Chem.* 19 (2013) 161–165.
- [33] M. Montazerzohori, M.H. Habibi, S. Joohari, V. Khodadostan, The effects of some operational parameters in photodegradation of benzylamine and aniline and their kinetics in aqueous suspension of TiO₂ and Pt-loaded TiO₂, *Annal. Chim.* 97(10) (2007) 1015–1026.
- [34] M. Montazerzohori, M. Nasr-Esfahani, S. Nezami, S. Mojahedi, Kinetic studies of photocatalytic decomposition of Eriochrome black T in buffer solutions at various pHs under high pressure mercury lamp irradiation, *Fresenius Environ. Bull.* 20 (2011) 1836–1840.
- [35] M. Montazerzohori, S. Nezami, S. Mojahedi, A kinetic study of photocatalytic degradation of tolonium chloride under high pressure irradiation in aquatic buffer systems, *E-J. Chem.* 8(S1) (2011) S19–S26.
- [36] M. Montazerzohori, M. Nasr-Esfahani, S. Mojahedi Jahromi, A. Malekhoseini, Investigation of thionine photodecolorization kinetics in the presence of nano-titanium dioxide at various buffer media, *Fresenius Environ. Bull.* 21(6) (2012) 1422–1426.
- [37] M. Montazerzohori, M. Nasr-Esfahani, S. Joohari, Photocatalytic degradation of an organic dye in some aqueous buffer solutions using nano titanium dioxide: A kinetic study, *Environ. Protect. Engin.* 38 (2012) 45–55.
- [38] N. Guetta, H. Ait Amar, Photocatalytic oxidation of methyl orange in presence of titanium dioxide in aqueous suspension. Part I: Parametric study, *Desalination* 185 (2005) 427–437.
- [39] S. Mozia, M. Tomaszewska, A.W. Morawski, Photocatalytic degradation of azo-dye acid red 18, *Desalination* 185 (2005) 449–456.
- [40] C.M. So, M.Y. Cheng, J.C. Yu, P.K. Wong, Degradation of azo dye Procion red MX-5B by photocatalytic oxidation, *Chemosphere* 46 (2002) 905–912.
- [41] R. Sushil Kanel, R. Souhail Al-Abed, Influence of pH on the transport of nanoscale zinc oxide in saturated porous media, *J. Nanopart. Res.* 13 (2011) 4035–4047.
- [42] B. Junny, P. Pichat, Determination of the actual photocatalytic rate of H₂O₂ decomposition over suspended TiO₂, *Langmuir* 7 (1991) 947–954.
- [43] I. Langmuir, The mechanism of the catalytic action of platinum in the reactions, *Trans. Faraday Soc.* 17 (1921) 621–654.
- [44] R.W. Matthews, Photocatalytic oxidation and adsorption of methylene blue on thin films of near-ultraviolet-illuminated, *J. Chem. Soc. Farad. Trans.* 1, 85 (1989) 1291–1302.